Significant relaxivity gap between a low-spin and a high-spin iron(II) complex of structural similarity: an attractive off–on system for the potential design of responsive MRI probes†

Vitalie Stavila,‡[a] Mustapha Allali,[a] Laurence Canaple,[b] Yvon Stortz,[a] Cécile Franc,[a] Philippe Maurin,[a] Olivier Beuf,[c] Olivier Dufay,[a] Jacques Samarut,[b] Marc Janier[d] and Jens Hasserodt*[a]

Received (in Montpellier, France) 3rd October 2007, Accepted 16th November 2007
First published as an Advance Article on the web 4th December 2007
DOI: 10.1039/b715254j

We have identified a pair of structurally similar iron complexes in the oxidation state II that exist in a low-spin and a high-spin electronic spin state in aqueous media, respectively. The low-spin, diamagnetic complex (LS, **1**) is mute in MRI while the high-spin, paramagnetic complex (HS, **2**) generates considerable contrast in MRI. These results demonstrate that iron(II) complexes, hitherto neglected for contrast enhancement in MRI, have potential for the design of an MRI probe that suffers passage from one state to the other under the influence of a targeted biochemical activity and thus operates in an off–on mode. At 300 MHz (proton resonance frequency at 7 T field strength) and in phosphate buffer, we found a longitudinal relaxivity ($r1$) of 1.29 mM^{-1} s^{-1} for **2** that, in light of the difference in unpaired electrons of the central metal atoms (4 for Fe^{II}; 7 for Gd^{III}), comes remarkably close to that of gadolinium(III)–DOTA (2.44 mM^{-1} s^{-1}), a commercialized MRI contrast agent. Since gadolinium complexes are always paramagnetic and can therefore not be muted in MRI, the here presented Fe(II)-based system offers an alternative strategy to develop responsive MRI probes.

Introduction

The field of molecular imaging is currently experiencing an enormous expansion.[1,2] Particular attention is being paid to *in vivo* imaging methods in view of the enormous prospects of these techniques for developmental biology, the phenomenon of ageing, cancer research, or for the pharmacological profiling of drug candidates.[3,4] The *in vivo* monitoring of gene expression is essential for all these endeavours.[5]

Magnetic resonance imaging (MRI) is widely recognized as the soft-tissue imaging technique with superior spatial resolution (compared to positron emission tomography, PET) and for its lack of any depth-penetration limits (compared to optical imaging methods).[3,4] Two further fundamental technological differences between MRI and PET shall be put forth here: (a) MRI's low signal intensity, which makes the application of millimolar concentrations of (passive, high-relaxivity) paramagnetic contrast agents desirable, while PET enjoys excellent sensitivity at sub-micromolar tracer concentrations, and (b) the intrinsic impossibility to design PET tracers that pass from low to high signal intensity (or *vice versa*) upon chemical modification.

A completely independent way of how signal intensity is maximized in molecular and cell biology and biotechnology is by the use of *enzymatic amplification*. Applications of this strategy are numerous, but a few can be named here, such as the use of reporter genes that encode for glycosidases, phosphatases or oxidoreductases, or of enzyme-linked binding assays such as ELISA. Molecular probes for these enzymatic activities usually generate an optical signal, either chromogenic or fluorescent. This precludes their application to one of the most powerful tomography methods, MRI, for which the image contrast is based on the variation in relaxation times that water protons experience in different tissue types. Paramagnetic MRI contrast agents are often intravenously administered and passively bio-distributed according to various tissue properties. By far the majority of these agents are coordination complexes of the trivalent rare earth metal (lanthanide) gadolinium[6] that exhibits one of the highest magnetic susceptibilities of all elements due to its seven unpaired electrons and a favorable electronic relaxation time that allows for efficient "communication" with water protons and thus the effective enhancement of their relaxation rate.[7] However, gadolinium complexes, as well as other well-established types of contrast agents such as macromolecular iron oxide clusters, do not lend themselves to the transformation into an enzyme-responsive probe that *does not* influence the relaxation time of its environment *before* encountering the

[a] *Laboratoire de Chimie, UMR CNRS 5182, Université de Lyon-ENS, 46 allée d'Italie, 69364 Lyon, France. E-mail: jens.hasserodt@ens-lyon.fr; Fax: +33 472 72 88 60; Tel: +33 472 72 83 94*
[b] *Institut de Génomique Fonctionnelle de Lyon, Université de Lyon-ENS, France*
[c] *CREATIS-LRMN, UMR CNRS 5220, INSERM U630, Université de Lyon-UCB, Villeurbanne, France*
[d] *ANIMAGE, bat. CERMEP, 59 boulevard Pinel, 69003 Lyon, France*

† Electronic supplementary information (ESI) available: IR spectra and LCMS analyses of complexes **1** and **2**; details of the X-ray structural analysis. See DOI: 10.1039/b715254j

‡ Current address: Dpt. of Chemistry, Rice University, Houston, Texas, USA.

enzyme. In effect, gadolinium(III)-containing compounds will always generate a paramagnetic field due to gadolinium's seven unpaired electrons. A few attempts have been reported to minimize this effect by judicious design of the multi-dentate ligand.[8,9] This ligand has to be susceptible to chemical/biochemical modification and, in the process, should alter, to a certain degree, the relaxation-modifying properties of the central gadolinium atom.

It is however well established that a considerable fraction of the observed relaxivity of any given Gd complex is due to a phenomenon called outer-sphere relaxation, which cannot be suppressed by any means of molecular design; "in no case can the outer-sphere component be ignored...".[10] Hence, any enzyme-responsive agent based on gadolinium is necessarily MRI active in the absence of the enzyme and will therefore contribute to image contrast according to its passive biodistribution pattern. The actual image obtained would thus be the result of the superposition of the former image with that resulting from the activation of the probe according to the distribution of the targeted enzyme. This will always risk rendering the results ambiguous and difficult to judge by the biologist or radiologist.

The phenomenon that certain transition metals can exist in a low-spin (LS) or high-spin (HS) electronic state appears therefore particularly attractive as a starting point for the design of a bio-active MRI probe that changes its spin state upon encounter of the enzyme.[11] As has been long established, manganese, iron and cobalt (among others) can exist in their complexes either in the HS or LS state. However, only in the case of iron has there been found a comparable number of mono-nuclear coordination complexes in the LS and in the HS state, respectively. And in particular, iron(II) LS complexes are *diamagnetic* due to their even-numbered electron configuration (d_6), and thus should not, to any extent, alter the proton relaxation properties of their environment.

Of course, such a design is not limited to the case of iron(II) but may easily be envisaged for iron(III) as well, with the important difference that the latter benefits from a longer, more MRI-favorable electronic relaxation correlation time (1–100 ps for high-spin Fe(III) complexes;[12] for comparison: 100–1000 ps for Gd-based complexes;[10] ~1 ps for high-spin iron(II)[13,14]) but may not exist in a low-spin, diamagnetic configuration.

Although iron-based contrast agents are not new to the MRI community,[15] the real-world application of entities, either molecular or particular, based on its oxidation state II, have not yet surfaced. On the whole, mono-nuclear complexes of iron(II) have been ruled out for their unfavorable electronic relaxation time compared to gadolinium(III),[16] iron(III) and manganese(II). Iron(III) thus enjoyed and still enjoys some attention for niche applications in MRI.[12,17]

In a very rare case has an iron(II) spin-crossover complex been investigated for its $T1$-reducing properties in aqueous (deuterated) solution.[18] Studying a ternary iron(II) complex containing two tris(triazolyl)borato ligands, the authors observed an increasing tendency to reduce $T1$ with increasing temperature of the aqueous sample, thus demonstrating the awakening relaxivity resulting from a growing high-spin population of the complex. However, in light of the closed coordination shell provided by the two tris(triazolyl)borato ligands its absolute $r1$ values must remain inferior to iron(II) complexes with a water molecule in the first coordination sphere.

Attempts to evaluate iron-based compounds *in vitro* for their potential as a relaxation-enhancing agent in MRI include (a) an Fe_8 cluster ($[(tacn)_6Fe_8(\mu_3\text{-}O)_2(\mu_2\text{-}OH)_{12}]Br_8{\cdot}9H_2O$) displaying a high-spin ground state ($S = 10$),[19,20] and (b) polymeric particles of iron(II) with triazole/aminotriazole, originally studied as spin-transition materials.[21] The latter have been proposed as $T2$-reducing *thermosensible* systems exploitable in MRI.[22] Since their polymeric structure is lost in water, their *in vivo* application would necessitate coating as seen in $T2$-reducing SPIO particle contrast agents.

Lately, metal-directed self-assembly, a widely used methodology in supramolecular chemistry,[23,24] has been applied to the formation of high-molecular weight, high-relaxivity gadolinum-based contrast agents.[25] Specifically, the well-known selectivity and intensity of self-assembly to an iron(II) bispyridine quaternary complex has been exploited. This led to a "metallo-star" with significantly elevated relaxivity. It has to be stressed that the iron aspect of such an approach is purely structural and the resulting iron complex unit is low-spin and diamagnetic.

Any ferrous or ferric system that could be envisaged to allow the passage from a low-spin to a high-spin complex by a simple chemical modification, such as triggered by an enzymatic activity, will require the use of high field-strength ligands characterized by the almost exclusive presence of nitrogen donor sites. The resulting Fe^{II}/Fe^{III} redox couples of the corresponding complexes are known to show rather positive redox potentials ($> +0.50$ V).[26,27] Entry into the cytoplasm (the site of gene expression) of a low-spin iron(III) complex containing an all-nitrogen ligand may likely trigger a redox reaction in view of the established redox potential of -0.20 to -0.24 V reigning in the cell.[28] For these reasons, a system based on iron(II) appears to be initially preferable.

A thorough literature search has identified the macrocyclic iron(II) complexes $[Fe^{II}(tptacn)](ClO_4)_2$ **1**[26,29] and $[Fe^{II}(dptacn)(Cl)](PF_6)$ **2**(Cl)[30] (Scheme 1) as promising candidates for the design of a bio-active MRI contrast agent that does not modify the relaxation properties of its environment before encounter of the biochemical activity (off–on mode). However, complexes **1** and **2** have only been systematically characterized

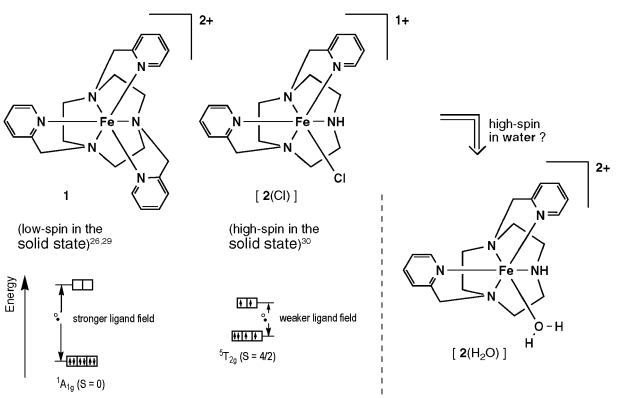

Scheme 1

in the solid state as potential spin-transition materials.[31,32–39] Their magnetic and relaxometric properties in solution,[40] particularly in water, are thus not known. This article describes an improved synthesis of the ligand dptacn **5**, its solid state structure (X-ray) in its mono-hydrochloride form, and the comparative magnetic, relaxometric, redox (UV-Vis), and MRI characterization in various aqueous media of complexes $[Fe^{II}(tptacn)][BF_4]_2$ **1** and $[Fe^{II}(dptacn)(H_2O)][BF_4]_2$ **2**(H_2O).

Results and discussion

Synthesis

Tptacn was resynthesized according to a literature procedure.[29] For the synthesis of dptacn **5** two new routes were explored since the published synthesis[41] turned out to be low-yielding and led to difficult-to-separate product mixtures. Route 1 (Scheme 2, **3** → **4** → **5**) starts from tri-tosylated tacn **3**[42,43] by removing two tosyl groups with satisfactory selectivity using HBr in glacial acetic acid.[44,45] Introduction of two picolyl groups yields compound **4** that is purified to homogeneity by silica gel chromatography. The last tosyl group is then removed by treatment with refluxing concentrated sulfuric acid for 34 h (see for example ref. 46).

These extremely harsh and oxidative conditions lead to extensive darkening of the sample, and after work-up a dark-brown oil is obtained that contains **5**. An attempt to isolate **5** consists of the precipitation of the hydrobromide of **5** by bubbling gaseous HBr into a CH_2Cl_2 solution of the oil. This procedure precipitates simultaneously a brown oily resin and a light-brown powder. The latter can be separated, and the free amine can be recovered by its treatment with NaOH and toluene in a Dean–Stark apparatus. The yield of this method starting from pure **4** is far from quantitative (28% over 3 steps). However, by applying this purification sequence we were able to obtain a sample so pure that

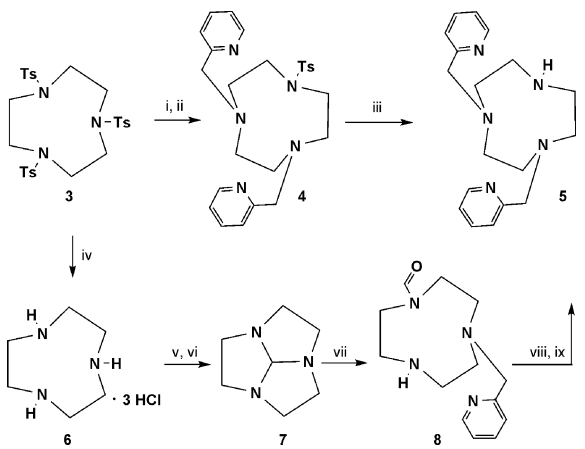

Scheme 2 (i) HBr 33% in AcOH, glacial AcOH, 90 °C, 30 h, then NaOH; (ii) 2-picolyl chloride hydrochloride (2.2 eq.), K_2CO_3 (7.3 eq.), MeCN, 50 °C, 36 h; (iii) H_2SO_4, 100 °C, 34 h then KOH, 0 °C until pH = 12; (iv) H_2SO_4, 150 °C, 10 min then MeOH, H_2O, 100 °C then HCl; (v) NaOH, toluene, H_2O, Dean–Stark; (vi) DMF dimethyl acetal (1 eq.), $CHCl_3$–toluene, 70 °C, 1 h; (vii) 2-picolyl chloride (0.95 eq.), THF, 0 °C, then 7 d at RT, then H_2O and reflux for 5 h; (viii) K_2CO_3 (7.3 eq.), dry MeCN, 2-picolyl chloride hydrochloride (1.07 eq.), 3 d, RT, (ix) KOH (3 eq.), EtOH, 110 °C, 24 h.

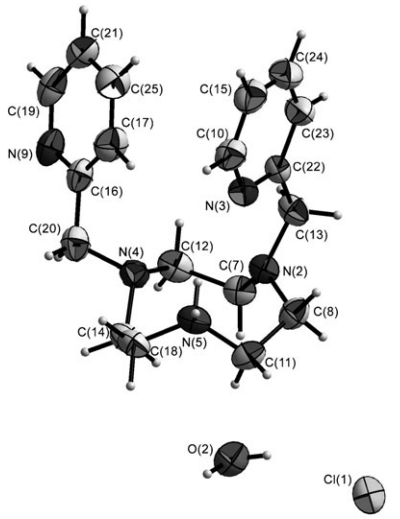

Fig. 1 Thermal ellipsoids plot of the asymmetric unit of **5** in its mono-hydrochloride form (CCDC reference number 662473. For crystallographic data in CIF or other electronic format see DOI: 10.1039/b715254j), with ellipsoids drawn at the 30% probability level. The asymmetric unit also contains a water molecule.

it crystallized from a benzene solution as the free penta-amine **5** (Fig. 1).

In view of the considerable amounts of this ligand required for future studies (chemical and biological), we turned to another method based on *N*,*N*,*N*-orthoacetal formation that has been briefly described in 1987 for the formation of mono-benzylated tacn.[47] This elegant strategy of forming aminals for selective introduction of alkyl chains has since been successfully applied to various macrocyclic systems bearing a number of nitrogen atoms equal to and in excess of three (see for example ref. 48–50). The synthetic sequence starts with the generation of the free base from the hydrochloride of tacn **6**. This is accomplished by refluxing **6** in toluene in the presence of conc. NaOH in a Dean–Stark apparatus. The pure tacn, crystallizing at 4 °C, is then treated with the dimethyl acetal of DMF to furnish *N*,*N*,*N*-orthoacetal **7**. Compound **7** is introduced into the first alkylation step without purification. Treatment with picolyl chloride in THF over 7 days leads to the precipitation of the ammonium salt. This salt is refluxed in water in order to obtain the formylated mono-alkylated tacn **8**. This product is introduced into the second alkylation without further purification. The resulting formylated precursor of dptacn is purified to homogeneity by silica gel chromatography. It is obtained with a yield of 62% over four steps starting from tacn hydrochloride **6**. Finally, the formyl group is removed by base hydrolysis over 24 h to furnish dptacn **5** in 95% yield. Optimization efforts for route 2 should lead to even higher yields. We now apply this elegant method[47] to the synthesis of various tacn derivatives bearing two to three *different* pendant arms with excellent results.

The use of a different counterion notwithstanding, Fe^{II} complexes **1** and **2** were obtained through literature protocols by precipitation upon addition of $[Fe(H_2O)_6][BF_4]_2$ to degassed methanol and acetonitrile solutions of dptacn[30] and tptacn,[26,29] respectively.

Table 1 Magnetic moments in solution (determined by Evans' method) and comparison to published values determined in the solid state

	μ_{eff}/μ_B (solvent) (295 K)	μ_{eff}/μ_B in the solid state (295 K)
1	0.9 (D_2O) 0.9 (CD_3CN) 0.9 (CD_3OD)	0.20–0.63 [Fe(tptacn)]$(ClO_4)_2$[26,29]
2	5.5 (D_2O) 4.7 (CD_3CN) 4.8 (CD_3OD)	5.04 [Fe(dptacn)(Cl)](PF_6)[30]
3	nd	3.58 [Fe(dptacn)(Cl)]$(PF_6)_2$[53]
4	nd	2.71 [Fe(tptacn)]$(ClO_4)_3$[26]

Determination of magnetic moments in solution (Evans' method)

Six-coordinate iron(II) complexes may be diamagnetic ($^1A_1$, LS), paramagnetic, ($^5T_2$, HS), or exhibit a temperature-induced LS ⇔ HS transition that depends on the relative magnitude of crystal field strength of the ligand and the mean electron-pairing energy.[32–38] The magnetic moments of complexes **1** and **2** were determined in solution by Evans' method.[51,52] In MeOH, MeCN and H_2O, **1** was found to be diamagnetic at room temperature (with a residual paramagnetism due to the temperature-independent paramagnetism), while **2** is paramagnetic in these solvents (Table 1). The obtained magnetic susceptibilities prove that the high-spin electronic state of **2** is preserved when passing from the solid to the liquid state.

By contrast, and for comparison, iron(III) complexes of these two ligands (**3** and **4**) show only a very slight difference in magnetic susceptibility in the solid state. While paramagnetic **4** shows a magnetic moment typical of low-spin iron(III) (one unpaired d electron),[26] **3** was determined to be a spin-crossover complex that exists at room temperature in a thermal equilibrium of the high-spin and low-spin forms.[53] Aside from the fact that such a feeble difference appears to be of no interest for the design of bio-activatable contrast agents, it should be stressed that the two here discussed penta- and hexa-nitrogen ligands very likely give much more stable complexes with iron(II) than with iron(III); in fact, a comparable penta-nitrogen ligand complexed with iron(III), when dissolved in acetonitrile and thus complexed with a sixth, high-field strength, nitrogen ligand, turned out to oxidize the solvent in order to attain the oxidation state +II![54] The stabilization of the +II oxidation state of [Fe(dptacn)X] in an aqueous environment should be less pronounced but is expected to be sufficient under cytoplasmic redox conditions (see below).

Fig. 2 shows the proton NMR spectra in D_2O of [Fe(tptacn)]$(BF_4)_2$ (at 300 K). The signals of the complex do not show any appreciable variation from the habitual chemical shifts, neither was any duplication of the solvent peaks observed, which adds to the Evans data in confirming the diamagnetic nature of **1**. The ensemble of the multiplet signals is in accord with spectra from other complexes with tptacn.[55,56] By contrast, and as expected, no spectrum in the habitual chemical shift interval could be obtained for high-spin complex **2**.

Proof-of-concept: relaxivity and the "off–on" effect

The influence on the longitudinal relaxation time ($T1$) of water protons was measured for samples of **1** and **2** at four different

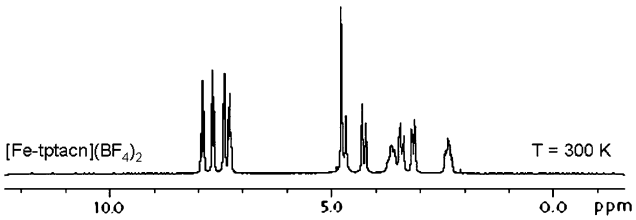

Fig. 2 ^1H NMR spectrum (D_2O) of **1**.

concentrations (ranging from 0.5 mM to 4 mM) in pure water, phosphate buffer (PB), phosphate-buffered saline (PBS), and serum, respectively (Fig. 3). In all media tested (only water shown), low-spin complex **1** showed no influence on $T1$. A solution of high-spin complex **2** in pure water, adjusted to pH 7, shows relaxation times comparable to those in phosphate buffer. In the (favorable) case of a concentration of 4 mM, these may amount to just 10% of the $T1$ found for solutions containing low-spin complex **1**, or, in other words, the native $T1$ value of the respective tissue under scrutiny (see also Fig. 4). This value compares rather well with the 5% found for Dotarem (Gd–DOTA) at the same concentration and conditions. That metal ions with lower magnetic moments than Gd^{III} can compete astonishingly well with gadolinium-based complexes has recently been demonstrated for Mn^{II} (five unpaired electrons).[57]

Importantly, aqueous samples of **2** synthesized either in MeOH or MeCN led to identical $T1$ values, thus indicating that any coordinating acetonitrile molecule was replaced by water. Significantly, in phosphate buffer containing considerable amounts of salt (NaCl), or in serum, longer relaxation times were measured. This observation may be explained with the elevated tendency of strongly cationic **2** to coordinate chloride rather than water at the sixth coordination site and thus reducing the $T1$-lowering capacity of **2**. Consequently, the $T1$ value found for Dotarem, itself being a gadolinium-based, mono-anionic complex, does not suffer as greatly from the

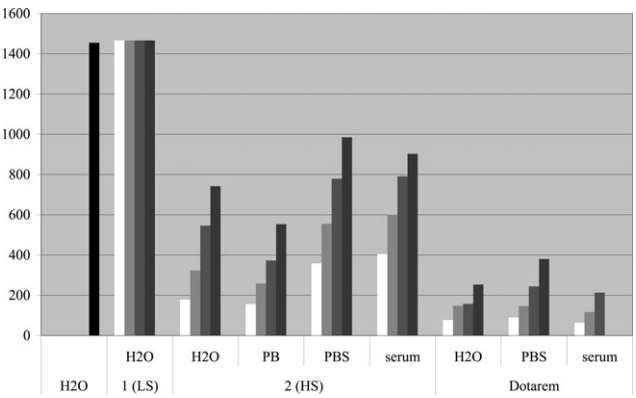

Fig. 3 Longitudinal relaxation times ($T1$/ms, room temperature) of pure water (black), [Fe(tptacn)][BF_4]$_2$ (**1**), [Fe(dptacn)][BF_4]$_2$ (**2**), and Dotarem® as reference. A series of concentrations (4.0, 2.0, 1.0, 0.5 mM, from white to dark grey, respectively) was measured. Solutions were prepared and measured under strictly anaerobic conditions. The H_2O solution of **2** was adjusted to pH = 7 by addition of 0.1 N NaOH. PB and PBS solutions (pH 7.4) contain 10 mM phosphate buffer and an additional 137 mM NaCl in the case of PBS.

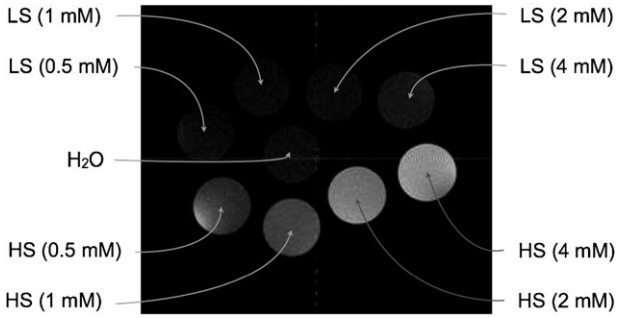

Fig. 4 *T*1-weighted MR images of tubes containing [Fe(tptacn)][BF_4]$_2$ (**1**, LS), and [Fe(dptacn)][BF_4]$_2$ (**2**, HS), at a series of concentrations (4.0, 2.0, 1.0, 0.5 mM). Reference: tube containing pure water.

presence of high salt concentration. In order to test this explanation, the synthesis of neutral analogues of **2**, that will however ensure establishment of the low-spin state in the presence of a third arm, is currently underway in our laboratory.

Fig. 4 illustrates the difference in contrast obtained in an MRI experiment of aqueous samples of the LS and HS complex, contained in tubes placed in the research tomograph. The image has been reconstructed with an IR-FISP sequence (inversion-recovery fast imaging with steady-state precession) with 1168 ms *T*1.

Redox properties (UV analysis)

Low-spin complex **1** shows no spectral signs for oxidation under air. Conversely, the spontaneous oxidation reaction of **2** under air can be conveniently followed by UV analysis, though UV spectroscopy does not provide unequivocal proof for a particular oxidation state (Fig. 5). During the reaction, the band characteristic for **2** at 388 nm[30] decreases in intensity, while the only reaction product exhibits an electronic absorption spectrum with a major band at 303 nm including a shoulder at 335 nm and a broad band between 490 and 560 nm. These bands do not correspond to the ones found for the iron(III) complex [Fe(dptacn)(Cl)][PF_6]$_2$ in acetonitrile (530 (sh) (280), 428 (1760), 251 (12 070)).[53] It should be noted, however, that the oxidation of the central atom would have resulted in only a shift of the wavelength of the absorption bands with little change in the spectral structure or band shape.[58]

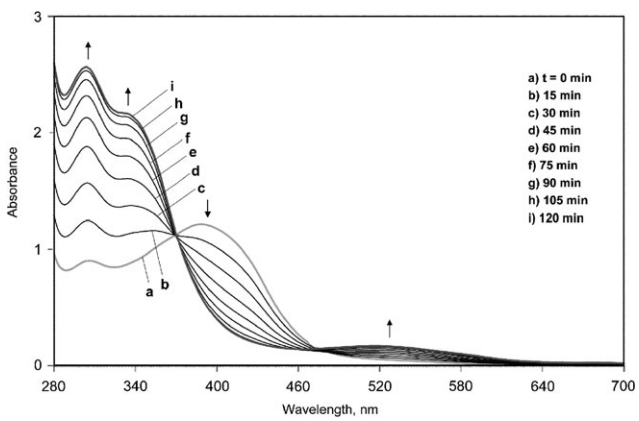

Fig. 5 UV-vis monitoring of the reaction of [Fe(dptacn)][BF_4]$_2$ with dioxygen in water. Two isosbestic points at 471 and 370 nm are observed.

Formation of oxo-bridged dinuclear species[54,59–61] cannot be ruled out in this oxidation reaction, but the cases of pentadentate mono-nuclear iron species where this behavior is absent may be explained with the steric crowding of the ligand.[62] §

The Fenton reaction,[63,64] frequently evoked in the context of the chemistry of iron complexes with free coordination sites, may as easily be observed in iron(II) species ([Fe^{II}–EDTA] and [Fe^{II}–DTPA]), as it is not ([$Fe^{II}(MGD)_2$] and [$Fe^{II}(DTCS)_2$]).[65–67] Any absence of a hydroxyl radical-generating capacity of complex **2** *in vitro* and *in vivo* thus remains to be determined.

An oxygen partial pressure-sensing complex based on the Eu^{II}/Eu^{III} redox pair has been reported.[68] This system is distinct from ours in that it behaves like an on–off system ($Eu^{II} \rightarrow Eu^{III}$ upon oxidation by O_2) and not *vice versa*. Also, the authors articulate their concern about stabilising the oxidation state of the initial Eu^{II} complex (the actual contrast agent, since Eu^{III} shows poor relaxivity). Our LS complex **1** benefits from a closed ligand shell of particularly elevated field strength which makes it stable to spontaneous oxidation even during mixing with air. Another oxygen-sensing complex based on the redox pair Mn^{II}/Mn^{III} and the tpps ligand (tpps = 5,10,15,20-tetrakis(*p*-sulfonatophenyl)porphinate) that was introduced as not being oxidation-sensitive in its initial state, actually exhibits a negligible difference in relaxivities when going to field strengths of 1.5 T and beyond (current trend in clinical tomograph design).[69] In any case, these systems, with potential merits in their own realm, do not compete with the here presented system. Our system may serve for the design of a complex whose ligand chemical constitution is altered by the action of a hydrolytic enzyme while the europium- and manganese-based complexes need to suffer oxidation of their central metal ion for contrast change.

Conclusion

In conclusion, this paper presents a pair of low-spin and high-spin ferrous complexes that are structurally so similar that they may serve as the basis for the design of an enzyme-responsive MRI probe with a true off–on nature.[11] In light of the fundamental differences with gadolinium-based systems, the here presented alternative path merits further exploration. The assessment of two independent candidates with the potential for enzymatic activation is currently underway.

Experimental

Materials and methods

MRI acquisition was performed on samples of different concentrations of complexes **1** and **2** using a 7 T Biospec system

§ One may point out that in a number of cases this oxidation reaction has been reported as the unsaturation of a nitogen–carbon bond and that this could be the case here, too. In our opinion, however, the absence of any possible conjugation of the newly formed double bond with an aryl system (usually a pyridyl group) and the lack of any literature precedent involving a tacn macrocyle do not concur with this view.

(Bruker, Ettlingen, Germany) associated with a 32 mm inner diameter bird cage coil (Rapid Biomedical, Würzburg, Germany). The longitudinal relaxation time $T1$ was measured with the IR-FISP sequence (inversion-recovery fast imaging with steady-state precession). Imaging parameters were: TR/TE = 4.2/2.1 ms, inversion times $TI = (68 + i \times 50)$ ms where $i = 0, 1, \ldots, 32$. Geometric parameters were: 40×40 mm^2 FOV, 5 mm slice thickness and 256×192 matrix size. $T1$ values were obtained from multiple TI images by fitting a mono-exponential function to the data.

LCMS analyses (see ESI†) were carried out on an AGILENT 1100 LCMSD (VL) system using ChemStation software, and a diode array detector (UV).

All reactions were conducted under an inert atmosphere using Schlenk tubes and vacuum-line techniques. Picolyl chloride hydrochloride and HBr (33%) in AcOH were obtained from Alfa Aesar; *N*,*N*′-dimethylformamide dimethyl acetal from Fluka.

1,4,7-Tris(*p*-toluenesulfonyl)-1,4,7-triazacyclononane (tacn(Ts)$_3$) **3** was synthesized according to a literature procedure.[42,43] THF and EtOH were freshly distilled, while AcCN, DMF, and pyridine were used as purchased.

Syntheses

1-(*p*-Toluenesulfonyl)-1,4,7-triazacyclononane. A stirred solution of tacn(Ts)$_3$ **3** (17.56 g, 29.7 mmol) and phenol (21.00 g, 223.0 mmol) is heated at 90 °C in 240 mL of HBr (33% in glacial acetic acid) for 30 h. A white precipitate appears after 3 h of heating. The reaction mixture is allowed to cool to room temperature and then filtered. The thus obtained hydrobromide is washed with diethyl ether (2×80 mL), then dissolved in 1 M NaOH until pH = 12 is reached, and finally extracted with diethylether (8×50 mL). The combined organic phases are dried with Na_2SO_4 and concentrated *in vacuo* to furnish a white solid (7.36 g, 88%) that is introduced into the next step without further purification. δ_H (200 MHz, $CDCl_3$) 7.67 (d, J = 8.2 Hz, 2H); 7.30 (d, J = 8.2 Hz, 2H); 3.37 (s, 3H); 3.18 (dt, J = 19.6 Hz, J = 2.0 Hz, 6H); 2.97 (s, 3H); 2.41 (s, 3H).

1-(*p*-Toluenesulfonyl)-4,7-di(picolyl)-1,4,7-triazacyclononane (4). 2-Picolylchloride hydrochloride (4.30 g, 26.2 mmol) is added to a stirred suspension of 1-(*p*-toluenesulfonyl)-1,4,7-triazacyclononane (3.37 g, 11.89 mmol) and K_2CO_3 (12.00 g, 86.83 mmol) in 60 mL of dry acetonitrile under inert atmosphere. After 36 h at 50 °C the residual solid is filtered, washed with acetonitrile (2×10 mL) and the combined organic phases concentrated *in vacuo*. Purification of the crude product by silica gel chromatography (CH_2Cl_2–MeOH 15 : 1 to 5 : 1) gives the pure 1-(*p*-toluenesulfonyl)-4,7-di(picolyl)-1,4,7-triazacyclononane as a yellow oil (2.80 g, 54%); δ_H (200 MHz, $CDCl_3$) δ 8.49 (d, J = 4.8 Hz, 2H); 7.63 (m, 4H); 7.47 (d, J = 7.8 Hz, 2H); 7.26 (d, J = 6.2 Hz, 2H); 7.13 (t, J = 4.8 Hz, 2H); 3.90 (s, 4H); 3.19 (dd, J = 22.0 Hz, J = 6.4 Hz, 8H); 2.80 (s, 4H); 2.40 (s, 3H); δ_C (50 MHz, $CDCl_3$) 159.8; 148.8; 142.8; 136.2; 135.8; 129.4; 126.9; 123.1; 121.8; 63.6; 55.6; 50.7; 21.3.

1,4-Di(picolyl)-1,4,7-triazacyclononane (dptacn) (5). 1-(*p*-Toluenesulfonyl)-4,7-di(picolyl)-1,4,7-triazacyclononane (502 mg, 1.08 mmol) is dissolved in 5 mL of concentrated sulfuric acid and heated for 32 h at 100 °C. The reaction mixture is cooled to 0 °C and the pH adjusted to 12 by careful addition to a freshly prepared solution of 50% NaOH. The resulting mixture is extracted with chloroform (3×50 mL) and the combined organic extracts are dried over Na_2SO_4 and concentrated *in vacuo* to give a dark brown oil (255 mg, 76%). This crude dptacn (**5**) is then converted into its hydrobromide by bubbling HBr into a stirred CH_2Cl_2 solution of the isolated dark brown oil. The resulting suspension is concentrated on the rotavap to give a residue that is reprecipitated in a minimum amount of hot methanol to furnish a light brown powder (156 mg, 30%). Liberation of dptacn **5** from this HBr salt is achieved by refluxing its suspension in 1.6 mL of toluene–water (80 : 20) in the presence of 80 mg of crunched NaOH pellets in a Dean–Stark apparatus at 140 °C until complete recovery of the initially introduced water. The resulting suspension is filtered hot, the solid resuspended in 5 mL toluene in the presence of an additional 50 mg NaOH, and stirred for 10 min at 140 °C in the Dean–Stark apparatus. This suspension is again filtered hot, and the organic phases are combined and evaporated to give dptacn (**5**) as an orange dense oil (77 mg, 23% over three steps). δ_H (200 MHz, $CDCl_3$) 8.57 (d, 2H); 7.53 (t, 2H); 7.15 (dd, 4H); 3.85 (s, 4H); 3.15 (t, 4H); 2.95 (t, 4H); 2.65 (s, 4H); δ_C (50 MHz, $CDCl_3$) 157.2; 149.3; 136.7; 122.8; 122.5; 60.8; 52.6; 49.4; 45.2.

1,4,7-Triazacyclononane·3HCl (6). tacn(Ts)$_3$ **3** (15.00 g, 25.4 mmol) is added to 15 mL of conc. H_2SO_4 heated to 140 °C, and stirred for 10 min at that temperature. After cooling to RT, the viscous clear solution is added dropwise to 70 mL MeOH and stirred overnight to yield a finely dispersed beige solid. The solid is filtered, redissolved in 7.5 mL water heated to 100 °C, and, after cooling, treated with 7.5 mL conc. HCl to yield a white precipitate, which is washed two times with EtOH, and subsequently two times with ether (5.00 g, 83%). δ_H (200 MHz, D_2O) 3.42 (s).

1,4,7-Triazacyclononane (tacn). To a solution of **6** (3.28 g, 13.7 mmol) and solid NaOH (1.44 g, 35.7 mmol) in 5.7 mL of water is added a layer of 20 mL of toluene. This mixture is heated to reflux in a Dean–Stark apparatus in order to remove water completely. The toluene solution is decanted from the resin-like residue and the latter is refluxed with another batch of 4 mL of toluene and 775 mg NaOH for 2 h and then filtered hot. The organic phases are combined and concentrated *in vacuo*. The resulting oil is cooled to 4 °C overnight to give hygroscopic crystals of tacn (1.61 g, 91%). δ_H (200 MHz, $CDCl_3$) 2.75 (m, 12H); 1.88 (s, 3H).

1,4,7-Triazacyclo[5.2.1.0^{4,10}] decane (7). Tacn (500 mg, 3.9 mmol), dissolved in a minimum amount of $CHCl_3$, is treated with 5 mL of toluene and heated to 70 °C. *N*,*N*′-dimethylamino-dimethylacetal (465 mg, 3.9 mmol) is added, and the solution is stirred for 1 h at 70 °C. Solvents were evaporated under reduced pressure to lead to 1,4,7-triazacyclo[5.2.1.0^{4,10}] decane as a transparent oil (453 mg, 84%) that is introduced into the next step without further purification. δ_H (200 MHz, $CDCl_3$)5.00 (s, 1H); 3.03 (m, 6H); 2.76 (m, 6H).

1-Formyl-4-picolyl-1,4,7-triazacyclononane (8). Picolyl chloride is obtained as a bright red oil by dissolving its hydrochloride salt in dry AcCN at 50 °C for 4 h in the presence of 4 eq. of NaOH, followed by filtration through a pad of silica and removal of the solvent under reduced pressure.

A solution of *N*,*N*,*N*-orthoacetal **7** (250 mg, 1.8 mmol) in 9 mL of THF is treated dropwise with a solution of picolyl chloride (223 mg, 1.75 mmol) in 6 mL of THF and stirred at room temperature for 7 days. The reaction is monitored by taking up aliquots from the reaction mixture in a water–AcCN mixture and analysing them by LCMS. In case, residual **7** remains an additional amount of picolyl chloride is added. The solvent is removed *in vacuo* to give an orange oil that is refluxed 5 h in 7 mL of water. Subsequently, THF is removed on the rotavap and the aqueous solution is lyophilised to give **8** as a brown oil (406 mg) that is introduced into the next step without further purification.

1-Formyl-4,7-dipicolyl-1,4,7-triazacyclononane. A stirred solution of **8** (406 mg, 1.63 mmol) in 10 mL of dry AcCN is treated with K_2CO_3 (1.81 g, 13.1 mmol) and picolyl chloride hydrochloride (287 mg, 1.8 mmol). The reaction is monitored by LCMS and is usually complete in 3 days. Evaporation of the solvent and purification by silica gel chromatography (CH_2Cl_2–MeOH 15 : 1 to 10 : 1) gives the desired product as an orange oil (492 mg, 84%). δ_H (200 MHz, $CDCl_3$) 8.53 (m, 2H); 8.05 (s, 1H); 7.67 (m, 2H); 7.43 (m, 2H); 7.17 (m, 2H); 3.87 (d, 4H); 3.40(m, 2H); 3.26 (s, 4H); 3.02 (m, 2H); 2.80 (m, 2H); 2.58 (m, 2H). δ_C (50 MHz, $CDCl_3$) 163.5; 159.7; 159.5; 149.0; 148.8; 136.4; 136.2; 122.9; 122.7; 121.9; 63.7; 63.0; 57.8; 54.4; 54.2; 53.2; 50.3; 47.2.

1,4-Di(picolyl)-1,4,7-triazacyclononane (5). A stirred solution of 1-formyl-4,7-dipicolyl-1,4,7-triazacyclononane (110 mg, 0.32 mmol) in 3 mL of EtOH is treated with solid KOH (560 mg, 10 mmol). The resulting mixture is heated to reflux for 24 h, then neutralized by 1N HCl. The aqueous layer is separated and extracted with $CHCl_3$ (6 × 15 mL). The combined organic extracts are dried over Na_2SO_4 and concentrated *in vacuo* to give dptacn **5** as a yellow oil (95 mg, 95%). (NMR data identical to compound **5** produced by route 1.)

[Fe(tptacn)][BF_4]$_2$ (1). In a Schlenk flask $[Fe(H_2O)_6][BF_4]_2$ (0.454 g, 1.34 mmol) was dissolved in degassed MeOH (10 mL). To the resultant solution tptacn (0.541 g, 1.34 mmol) in the same solvent (10 mL) was added dropwise at room temperature. The resulting dark brown solution was stirred for 1 h, then stored overnight at 0 °C. This gave brown prismatic crystals that were collected in a filter, washed with diethyl ether (10 mL) and dried in vacuum to afford **1** (0.634 g, 75%). UV-Vis λ_{max} = 248 (3184) $\pi \rightarrow \pi^*$, 432 (11 970) MLCT; Anal. calcd for $C_{24}H_{30}N_6Fe(BF_4)_2$: C, 45.6; H, 4.8; N, 13.3. Found: C, 45.5; H, 4.8; N, 13.2. Chromatographic purity (LCMS) was proven by mass (ESI, LRMS) data and UV (DAD) detection.

[Fe(dptacn)(MeOH)][BF_4]$_2$ (2). To 3 mL of a solution of $[Fe(H_2O)_6][BF_4]_2$ (0.338 g, 1.0 mmol) in degassed MeOH was added 4 mL of a methanol solution containing 0.311 g (1.0 mmol) dptacn. The resulting brown solution was kept under an Ar stream for 24 h to concentrate the solution to approximately a half of the initial volume to give brown prismatic crystals of **2** which were collected by filtration, washed with diethyl ether (10 mL), and dried under vacuum (0.401 g, 74%, hygroscopic and air-sensitive). UV-Vis λ_{max} = 237 (3179) $\pi \rightarrow \pi^*$, 329 (2870) MLCT. Chromatographic purity (LCMS) was proven by mass (ESI, LRMS) data and UV (DAD) detection.

Acknowledgements

We thank Delphine Pitrat for valuable technical assistance and Dr Erwann Jeanneau, Université Claude Bernard Lyon 1, for the X-ray crystal structure analysis. Financial support from the French National Research Agency (contract no. ANR-05-EMPB 010-01), the CNRS (Imagerie du Petit Animal program), the French Ministry for Research, the Rhone-Alpes Genopole and EUMORPHIA (*via* ANIMAGE) is gratefully acknowledged.

References

1 V. Marx, *Chem. Eng. News*, 2005, **83**(30), 25–36.
2 S. Aime and R. N. Muller, *Contrast Media Mol. Imaging*, 2006, **1**, 1.
3 T. F. Massoud and S. S. Gambhir, *Genes Dev.*, 2003, **17**, 545–580.
4 M. Rudin and R. Weissleder, *Nat. Rev. Drug Discovery*, 2003, **2**, 123–131.
5 A. Bogdanov and R. Weissleder, *Trends Biotechnol.*, 1998, **16**, 5.
6 E. Toth and A. E. Merbach, *The Chemistry of Contrast Agents in Medical Magnetic Resonance Imaging*, Wiley, Chichester, 2001.
7 P. Caravan, J. J. Ellison, T. J. McMurry and R. B. Lauffer, *Chem. Rev.*, 1999, **99**, 2293–2352.
8 A. Y. Louie, M. M. Huber, E. T. Ahrens, U. Rothbacher, R. Moats, R. E. Jacobs, S. E. Fraser and T. J. Meade, *Nat. Biotechnol.*, 2000, **18**, 321–325.
9 J. A. Duimstra, F. J. Femia and T. J. Meade, *J. Am. Chem. Soc.*, 2005, **127**, 12847–12855.
10 R. B. Lauffer, *Chem. Rev.*, 1987, **87**, 901–927.
11 J. Hasserodt, *Int. Pat.*, WO2005094903, 2005.
12 N. Richardson, J. A. Davies and B. Raduchel, *Polyhedron*, 1999, **18**, 2457–2482.
13 I. Bertini, C. Luchinat and G. Parigi, *Solution NMR of Paramagnetic Molecules (Current Methods in Inorganic Chemistry)*, Elsevier, Amsterdam, 2006.
14 Y. Ducommun, K. E. Newman and A. E. Merbach, *Inorg. Chem.*, 1980, **19**, 3696–3703.
15 R. B. Lauffer, W. L. Greif, D. D. Stark, A. C. Vincent, S. Saini, V. J. Wedeen and T. J. Brady, *J. Comput. Assist. Tomogr.*, 1985, **9**, 431–438.
16 P. H. Fries, C. Gateau and M. Mazzanti, *J. Am. Chem. Soc.*, 2005, **127**, 15801–15814.
17 D. D. Schwert, N. Richardson, G. J. Ji, B. Raduchel, W. Ebert, P. E. Heffner, R. Keck and J. A. Davies, *J. Med. Chem.*, 2005, **48**, 7482–7485.
18 C. Janiak, T. G. Scharmann, T. Brauniger, J. Holubova and M. Nadvornik, *Z. Anorg. Allg. Chem.*, 1998, **624**, 769–774.
19 K. Wieghardt, K. Pohl, I. Jibril and G. Huttner, *Angew. Chem., Int. Ed. Engl.*, 1984, **23**, 77–78.
20 E. Rodriguez, A. Roig, E. Molins, C. Arus, M. R. Quintero, M. E. Cabanas, S. Cerdan, P. Lopez-Larrubia and C. Sanfeliu, *NMR Biomed.*, 2005, **18**, 300–307.
21 J. Krober, E. Codjovi, O. Kahn, F. Groliere and C. Jay, *J. Am. Chem. Soc.*, 1993, **115**, 9810–9811.

22 R. N. Muller, L. Vander Elst and S. Laurent, *J. Am. Chem. Soc.*, 2003, **125**, 8405–8407.
23 *Comprehensive Supramolecular Chemistry*, ed. J.-M. Lehn, J. L. Atwood, J. E. D. Davies, D. D. MacNicol and F. Vögtle, Pergamon Oxford, 1996.
24 J. M. Lehn, *Supramolecular Chemistry: Concepts and Perspectives*, VCH, Weinheim, 1995.
25 J. B. Livramento, E. Toth, A. Sour, A. Borel, A. E. Merbach and R. Ruloff, *Angew. Chem., Int. Ed.*, 2005, **44**, 1480–1484.
26 K. Wieghardt, E. Schoffmann, B. Nuber and J. Weiss, *Inorg. Chem.*, 1986, **25**, 4877–4883.
27 M. DiVaira, F. Mani and P. Stoppioni, *J. Chem. Soc., Dalton Trans.*, 1997, 1375–1379.
28 F. Q. Schafer and G. R. Buettner, *Free Radical Biol. Med.*, 2001, **30**, 1191–1212.
29 L. Christiansen, D. N. Hendrickson, H. Toftlund, S. R. Wilson and C. L. Xie, *Inorg. Chem.*, 1986, **25**, 2813–2818.
30 L. Spiccia, G. D. Fallon, M. J. Grannas, P. J. Nichols and E. R. T. Tiekink, *Inorg. Chim. Acta*, 1998, **279**, 192–199.
31 H. Toftlund and J. J. McGarvey, in *Spin Crossover in Transition Metal Compounds I*, ed. P. Gütlich and H. A. Goodwin, 2004, *Top. Curr. Chem.*, **233**, 151–166.
32 S. Cobo, G. Molnar, J. A. Real and A. Bousseksou, *Angew. Chem., Int. Ed.*, 2006, **45**, 5786–5789.
33 J. A. Real, A. B. Gaspar and M. C. Munoz, *Dalton Trans.*, 2005, 2062–2079.
34 A. Bousseksou, G. Molnar and G. Matouzenko, *Eur. J. Inorg. Chem.*, 2004, 4353–4369.
35 *Spin Crossover in Transition Metal Compounds I–III*, ed. P. Gütlich and H. A. Goodwin, *Top. Curr. Chem.*, 2004, **233–235**.
36 O. Kahn and C. J. Martinez, *Science*, 1998, **279**, 44–48.
37 P. Gutlich, A. Hauser and H. Spiering, *Angew. Chem., Int. Ed. Engl.*, 1994, **33**, 2024–2054.
38 E. König, G. Ritter and S. K. Kulshreshtha, *Chem. Rev.*, 1985, **85**, 219–234.
39 A. H. R. Alobaidi, J. J. McGarvey, K. P. Taylor, S. E. J. Bell, K. B. Jensen and H. Toftlund, *J. Chem. Soc., Chem. Commun.*, 1993, 536–538.
40 H. Toftlund, *Monatsh. Chem.*, 2001, **132**, 1269–1277.
41 G. A. Mclachlan, G. D. Fallon, R. L. Martin, B. Moubaraki, K. S. Murray and L. Spiccia, *Inorg. Chem.*, 1994, **33**, 4663–4668.
42 J. E. Richman and T. J. Atkins, *J. Am. Chem. Soc.*, 1974, **96**, 2268–2270.
43 A. E. Martin and J. E. Bulkowski, *J. Org. Chem.*, 1982, **47**, 415–418.
44 J. L. Sessler, J. W. Sibert and V. Lynch, *Inorg. Chem.*, 1990, **29**, 4143–4146.
45 R. C. Roemmele and H. Rapoport, *J. Org. Chem.*, 1988, **53**, 2367–2371.
46 A. J. Dickie, D. C. R. Hockless, A. C. Willis, J. A. McKeon and W. G. Jackson, *Inorg. Chem.*, 2003, **42**, 3822–3834.
47 G. R. Weisman, D. J. Vachon, V. B. Johnson and D. A. Gronbeck, *J. Chem. Soc., Chem. Commun.*, 1987, 886–887.
48 M. Koikawa, K. B. Jensen, H. Matsushima, T. Tokii and H. Toftlund, *J. Chem. Soc., Dalton Trans.*, 1998, 1085–1086.
49 M. Le Baccon, F. Chuburu, L. Toupet, H. Handel, M. Soibinet, I. Dechamps-Olivier, J. P. Barbiere and M. Aplincourt, *New J. Chem.*, 2001, **25**, 1168–1174.
50 M. Raidt, M. Neuburger and T. A. Kaden, *Dalton Trans.*, 2003, 1292–1298.
51 D. F. Evans, *J. Chem. Soc.*, 1959, 2003–2005.
52 E. M. Schubert, *J. Chem. Educ.*, 1992, **69**, 62–62.
53 G. D. Fallon, G. A. McLachlan, B. Moubaraki, K. S. Murray, L. Obrien and L. Spiccia, *J. Chem. Soc., Dalton Trans.*, 1997, 2765–2769.
54 A. K. Patra, M. M. Olmstead and P. K. Mascharak, *Inorg. Chem.*, 2002, **41**, 5403–5409.
55 G. D. Norante, M. Divaira, F. Mani, S. Mazzi and P. Stoppioni, *J. Chem. Soc., Dalton Trans.*, 1992, 361–365.
56 W. G. Jackson, J. A. McKeon, D. C. R. Hockless and A. C. Willis, *Inorg. Chem.*, 2006, **45**, 4119–4135.
57 S. Aime, P. L. Anelli, M. Botta, M. Brocchetta, S. Canton, F. Fedeli, E. Gianolio and E. Terreno, *JBIC, J. Biol. Inorg. Chem.*, 2002, **7**, 58–67.
58 A. B. B. Lever, *Inorganic Electronic Spectroscopy*, Amsterdam, 1984.
59 L. Duelund, R. Hazell, C. J. McKenzie, L. P. Nielsen and H. Toftlund, *J. Chem. Soc., Dalton Trans.*, 2001, 152–156.
60 J. M. Rowland, M. Olmstead and P. K. Mascharak, *Inorg. Chem.*, 2001, **40**, 2810–2817.
61 J. P. Lopez, F. W. Heinemann, A. Grohmann, O. Horner, J. M. Latour and G. Ramachandraiah, *Inorg. Chem. Commun.*, 2004, **7**, 773–776.
62 W. S. Szulbinski, P. R. Warburton, D. H. Busch and N. W. Alcock, *Inorg. Chem.*, 1993, **32**, 297–302.
63 D. H. R. Barton and B. Hu, *Pure Appl. Chem.*, 1997, **69**, 1941–1950.
64 C. Walling, *Acc. Chem. Res.*, 1975, **8**, 125–131.
65 Y. Katayama, N. Soh and M. Maeda, *ChemPhysChem*, 2001, **2**, 655–661.
66 S. Pou, P. Tsai, S. Porasuphatana, H. J. Halpern, G. V. R. Chandramouli, E. D. Barth and G. M. Rosen, *Biochim. Biophys. Acta*, 1999, **1427**, 216–226.
67 G. R. Buettner, L. W. Oberley and S. Leuthauser, *Photochem. Photobiol.*, 1978, **28**, 693–695.
68 L. Burai, E. Toth, G. Moreau, A. Sour, R. Scopelliti and A. E. Merbach, *Chem.–Eur. J*, 2003, **9**, 1394–1404.
69 S. Aime, M. Botta, E. Gianolio and E. Terreno, *Angew. Chem., Int. Ed.*, 2000, **39**, 747–750.